THE JOURNAL OF PHYSICAL CHEMISTRY C
A JOURNAL OF THE AMERICAN CHEMICAL SOCIETY

pubs.acs.org/JPCC

Article

Toward Understanding Structural Stability in Cu-Substituted $(Pr_{1-x}Nd_x)_2NiO_{4+\delta}$ by *in Situ* and *Operando* Studies

Published as part of The Journal of Physical Chemistry virtual special issue "Esther Sans Takeuchi Festschrift".

Emir Dogdibegovic, Christopher J. Wright, Yudong Wang, Qingsheng Cai, Yanxing Zhang,* Guang Tian,* Shuai Yang, Jinbo Yang, Barbara Marchetti,* and Xiao-Dong Zhou*

Cite This: https://doi.org/10.1021/acs.jpcc.2c04006

Read Online

ACCESS | Metrics & More | Article Recommendations

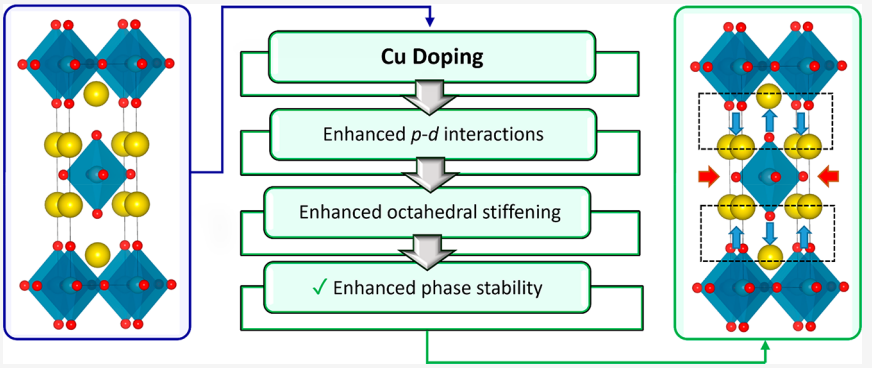

ABSTRACT: Praseodymium nickelates are promising materials to be used as an oxygen electrode in solid oxide cells. Phase transformation in these materials, however, is a major challenge, which may cause durability issues in a fuel cell or electrolyzer. There is a need to develop a strategy that allows researchers to construct an *in situ* phase-stable and active cathode material. The aim of this study is to complement our previous publications on the electrochemical properties of the $(Pr_{1-x}Nd_x)_2Ni_{1-y}Cu_yO_{4+\delta}$ series, which has shown an increased performance stability by 2 orders of magnitude when compared to bare $Pr_2NiO_{4+\delta}$. Systematic structural studies on a wide range of compositions were conducted *in situ via* long-term thermal annealing tests on powders. The structure–property relationship has been investigated using X-ray total scattering and atomic pair distribution function at a synchrotron source. In this work, we provide an attempt to identify a potential origin of structural stability and phase transition in praseodymium nickelates. A high temperature structure can be "frozen" preventing changes in M–O bond lengths, consequently leading to a stabilized structure. Results indicate that the two layers, associated with both Pr and Ni sites, are involved simultaneously in fully stabilizing the parent phase. Furthermore, it was found that Cu-doping on the Ni-site (in Pr_2NiO_4 structure) alone is not sufficient in stabilizing the parent phase. The structure and stability of the system were then investigated via density functional theory calculations, and computations of the density of states were undertaken for the Cu-doped and baseline compositions. It was found that *p*–*d* interactions, *i.e.*, oxygen–metal orbital interactions, were enhanced as Cu was used to dope the PNNO, thus increasing the structural stability of the material.

1. INTRODUCTION

Ruddlesden–Popper (RP) phases represent a novel class of oxides which have recently attracted increasing interest for various potential applications, including electrocatalysis. RP oxides can be described with the general formula $(A)_{n-1}(A')_2(B)_n(O)_{3n+1}$, where A, A′, and B are metal cations and n represents the number of the consecutive oxygen octahedron layers in the material, which are alternated with rock-salt-type layers (AO) along the c direction.[1,2] Among these oxides, the overstoichiometric $Pr_2NiO_{4+\delta}$ (PNO) was recently investigated as a promising oxygen electrode material for solid oxide cells, by virtue of its high oxygen-ion diffusion and surface exchange coefficients.[3−5] Interestingly, these properties are related to their ability to accommodate a large excess of oxygen, which distributes within the LnO rock-salt layer, in the $Ln_2NiO_{4+\delta}$ series, with Ln = La, Pr, or Nd.[3] Excess

Received: June 9, 2022
Revised: August 3, 2022

oxygen uptake in the stoichiometric Ln_2NiO_4 can be described in eq 1:[6]

$$Ln_2Ni^{2+}O_4 + \delta\frac{1}{2}O_2 \rightarrow Ln_2Ni^{2+}_{1-2\delta}Ni^{3+}_{2\delta}O_{4+\delta} \quad (1)$$

wherein the incorporation of interstitial oxygen aids to relieve structural stresses present in the stoichiometric compound by oxidation of Ni^{2+} into smaller Ni^{3+} ions, thus reducing strain in the otherwise compressed NiO_2 layers and, at the same time, favoring elongation of LnO distances.[7] The unique conduction behavior through oxygen interstitials in these overstoichiometric compounds has been investigated in detail in multiple reports.[5,8] Recent studies suggest that, as long as overstoichiometric oxygen is present, the apical oxide ions can undergo highly anisotropic thermal motion by migrating to the nearest-neighbor interstitial position (i.e., O3 site). The path of the diffusing oxygen ions was found to be curved in the $a-c$ plane as a result of repulsive interactions between Ln and O ions, which also maintain them at approximately constant distances.[5] Minervini et al.[9] calculated the oxygen migration in LNO using energy minimization techniques and found that the migration energy in the $a-c$ plane (0.29 eV) is 10× lower than in the b direction. These combined findings suggest that the presence of large cations of the Ln series can effectively enhance oxide conductivity within the rock-salt layer.[5] Furthermore, experimental electron density maps showed electron−hole conduction via B-site atoms in the Ni−O layer, indicating that the oxygen diffusion layer is accompanied by a two-dimensional electron−hole conductive layer.[10]

Nuclear and electron density distribution,[11] along with the theoretical valence electron density map, confirms the presence of interstitial O3 sites. The nuclear density at the O3 site was found to decease with an increase in temperature,[11] which is consistent with the decrease in occupancy factor at the O3 site and in the $4+\delta$ value in RP nickelates. The covalent bonds between the Ni-site ion (Ni, Cu, and Ga) and O1 atoms are observed on the 2D planes, while the (Pr,La) atoms are more ionic. The covalent bond on the Ni-site is formed by the overlap of Ni 3d, Cu 3d, and O1 2p orbitals, leading to a 2D network of B−O1. The oxygen overstoichiometry allows for unique oxygen ion conducting capabilities, which relate to high oxygen surface exchange and diffusion coefficients.[3,12,13]

With an increase in temperature the oxygen occupancy decreases, and different behavior in the curves can be linked to oxygen loss and phase transitions. Pr_2NiO_4 goes through subtle changes from Pr_2NiO_4 (n = 1) to $Pr_3Ni_2O_7$ (n = 2) and to $Pr_4Ni_3O_{10}$ (n = 3). Our recent work showed that Cu doping on the Ni-site in $(Pr_{0.50}Nd_{0.50})_2NiO_{4+\delta}$ (PNNO) electrodes resulted in stable long-term operation (nearly zero degradation), when compared to 6.4%/1,000 h degradation in PNO cells.[14] The aim of this study is to complement our previous publications on the electrochemical properties of the $(Pr_{1-x}Nd_x)_2Ni_{1-y}Cu_yO_{4+\delta}$ series,[14−18] by establishing the relationship between performance stability and structural behavior in $(Pr_{0.5}Nd_{0.5})_2Ni_{1-y}Cu_yO_{4+\delta}$ (PNNO-Cu$_y$), where y = 0.05, 0.10, and 0.20. As a result of manipulations on the Ni-site, changes in the oxygen octahedron layer were expected, but their role in the changes in the rock-salt layer was unknown. Detailed study of M−O bond length behavior was performed at room temperature and *in situ* at a synchrotron source, and the findings were used to correlate the structure, phase stability, and electrochemical stability. A strong correlation was found between the stiffening of the oxygen octahedra and shrinkage in rock-salt layer (oxygen ion conduction paths), leading to stabilized phase and stable electrochemical performance.

2. EXPERIMENTAL AND COMPUTATIONAL METHODS

Starting materials, including $Pr(NO_3)_3{\cdot}xH_2O$, $Nd(NO_3)_3{\cdot}xH_2O$, $Ni(NO_3)_2{\cdot}xH_2O$, and $Cu(NO_3)_2{\cdot}xH_2O$ (99.9% REO, Alfa Aesar, Haverhill, MA), were standardized using thermogravimetric analysis and were used in the glycine nitrate combustion process.[19] The synthesized powders were calcined in air with 3°/min heating and cooling rates. Single phase powders were studied via X-ray diffraction (XRD) analysis, using a Rigaku Miniflex II (Houston, TX) equipped with scintillating and high speed silicon strip (D/teX) detectors. Details on normalizing the flux and peak positions have been reported elsewhere and incorporated the use of multiple external and internal standards.[18] Rietveld refinement was performed using the FullProf code in orthorhombic *Bmab* symmetry.[20] Thermal annealing tests on powders were performed with 3% humidified air flow.

X-ray total scattering and *in situ* atomic pair distribution function (PDF)[21] analysis were performed at the Advanced Photon Source (APS), Argonne National Laboratory, beamline 11-ID-B. The high energy and high flux X-rays allowed detailed analysis of phase evolution in nickelates and their phase degradation products. The Ceria standard was used for detector and exposure calibration. An empty quartz tube (blank) was fixed in a flow furnace[22] (composed of a stainless-steel frame, heating elements, a quartz tube, heat shields, and thermocouples) and run through the entire temperature profile, providing the background for powder sample studies at all experimental conditions. A sample was then centered in front of a beam using a built-in camera and laser. Experimental data were collected via QXRD continuously at 86.7 keV and 25 cm detector distance for the PDF patterns. *In situ* studies ($T \leq$ 900 °C) were then performed in a controlled atmosphere, and respective data were continuously collected during heating and cooling. The data were processed using PDFgetX2 and in-house Python code. The background data were subtracted from the sample data. The analysis involved the pair distribution function (PDF) and Monte Carlo methods.

Supercells containing 56 atoms were constructed, and the self-consistent electronic structure calculations were performed for Pr_2NiO_4, $Pr_2Ni_{0.875}Cu_{0.125}O_4$, $PrNdNiO_4$, and $PrNdNi_{0.875}Cu_{0.125}O_4$ cathode materials. The calculations were carried out using the density-functional theory (DFT) method[17] as implemented in the Vienna *ab initio* simulation package VASP.[18] Projector augmented wave (PAW) pseudopotentials were used.[19] An energy cutoff of 400 eV and appropriate k-point meshes were chosen to ensure that the total energies are converged within 10^{-5} eV. Self-interactions and correlation effects due to localized 3d electrons have been addressed with the GGA+U method in its rotational invariant form.[20] Parameters of direct U and exchange J Coulomb interactions for Ni and Cu ions in the calculations were set to U_{Ni} = 7 eV, U_{Cu} = 8 eV, J_{Ni} = 0.6 eV and J_{Cu} = 0.95 eV, respectively, according to the values reported previously for similar cathode materials.[21,22] For Pr_2NiO_4 and $Pr_2Ni_{0.875}Cu_{0.125}O_4$, the total energy and electronic structure of both high temperature tetragonal (HTT) phase with space group $I4/mmm$ and low temperature orthorhombic (LTO) phase with space group *Bmab* were calculated with relaxation

https://doi.org/10.1021/acs.jpcc.2c04006
J. Phys. Chem. C XXXX, XXX, XXX−XXX

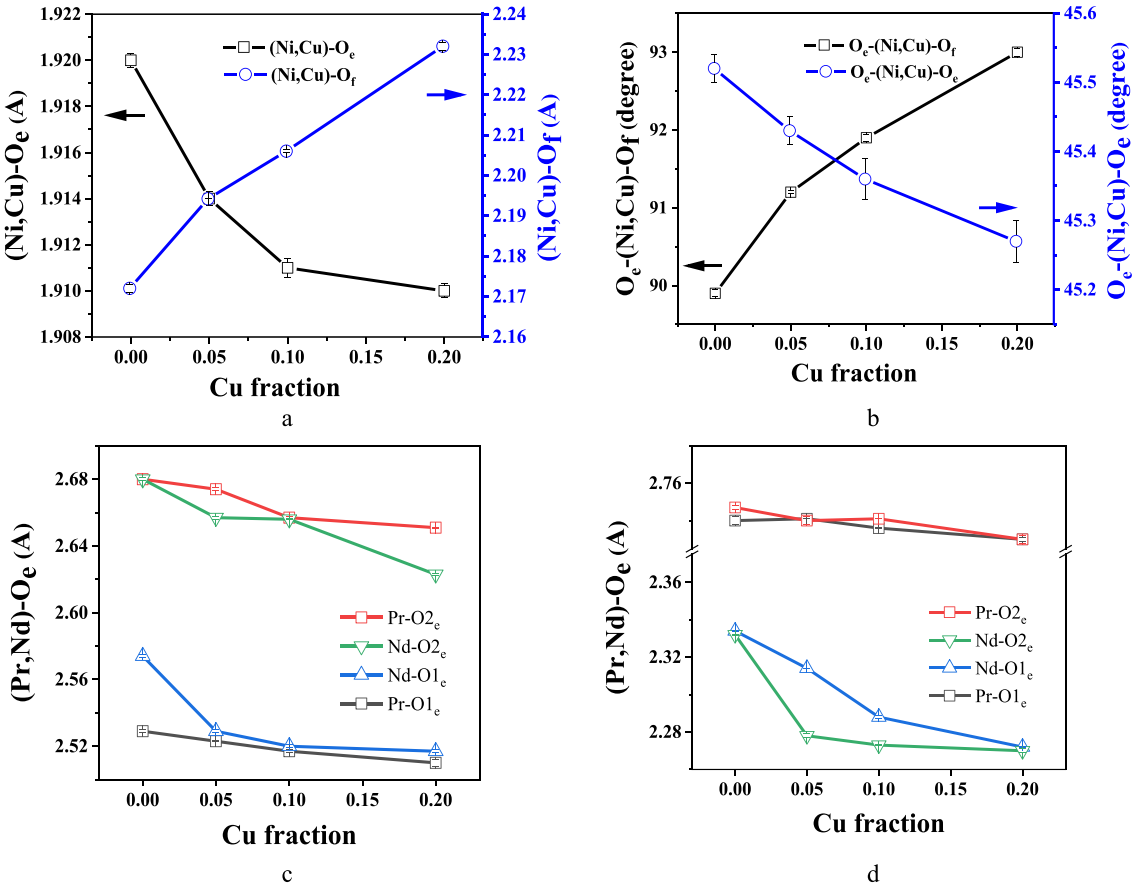

Figure 1. (a) Refined average (Ni,Cu)−O bond lengths for (Ni,Cu)O_e (equatorial) and (Ni,Cu)−O_f (focal) arrangements. (b) O−(Ni,Cu)−O bond angles for the same series. Refined average (Pr,Nd)−O bond lengths for (Pr,Nd)O_e (c), and (Pr,Nd)−O_f arrangements (d).

of both atomic positions and lattice parameters, while the calculations of $(Pr,Nd)_2NiO_4$ and $(Pr,Nd)_2(Ni_{0.875}Cu_{0.125})O_4$ were performed in the orthorhombic structure only, based on the lattice data from our experimental work.

3. RESULTS AND DISCUSSION

3.1. Structural Characterization at Room Temperature. The structural refinement on PNNO-Cu_y series, reported in our previous work,[17] showed an increase in the cell volume with increasing molar fraction of Cu, mainly driven by a 0.90% increase in the *c* lattice parameter. In addition, the fractional position coordinates on heavy metal cations (Pr, Nd) indicated an elongation in the *z* direction and overall compression in the *y* direction, while the orthorhombic *Bmab* symmetry was retained. In order to further investigate the role of Cu-doping on the crystal structure, the changes in lattice parameters were further studied by refinement of the average bond lengths in the perovskite and rock-salt layers.

Figure 1a shows the average (Ni,Cu)−O bond lengths for equatorial and focal oxygen positions (O_e and O_f, respectively) in the perovskite layer, represented with positions 1 and 2 (Figure 2a), respectively. The (Ni, Cu)−O_e bond length decreases by 0.30%, 0.40%, and 0.50% as the fraction of Cu is increased from 0.00 to 0.20; by contrast, the (Ni, Cu)−O_f increases by 2.80% across the range of Cu fraction explored, which is equivalent to 6-fold larger expansion in the focal direction. These results show that Cu doping within the oxygen octahedra forces equatorial oxygen atoms to arrange closer to the transition metal, which in turn creates steric strain

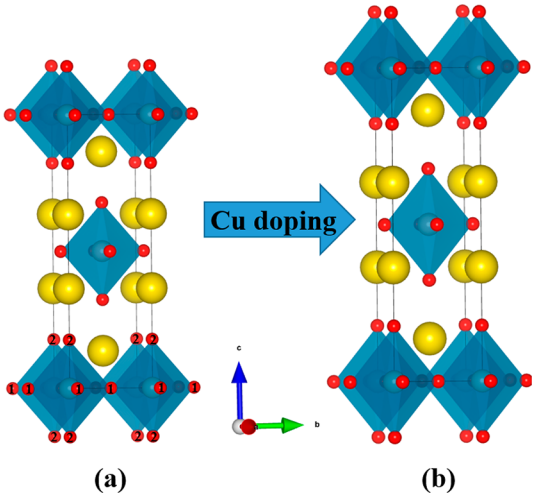

Figure 2. (a) Illustration showing the orthorhombic layered structure in $(Pr_{0.50}Nd_{0.50})_2NiO_{4+\delta}$ where perovskite layers (oxygen octahedral packed layer) alternate with the rock-salt M−O layers. (b) Resulting structural changes with Cu-doping on the Ni-site leading to increase in volume via expansion in the *z*-direction and shrinkage in the *a*−*b* plane. Shrinkage in oxygen ion conduction paths is highlighted. Yellow, red, and gray represent Pr or Nd, O, and Ni atom, respectively.

between equatorial and focal oxygen atoms and leads to repulsion of focal oxygen atoms toward the rock-salt layer. Furthermore, as shown by multiple studies on lanthanum

https://doi.org/10.1021/acs.jpcc.2c04006
J. Phys. Chem. C XXXX, XXX, XXX−XXX

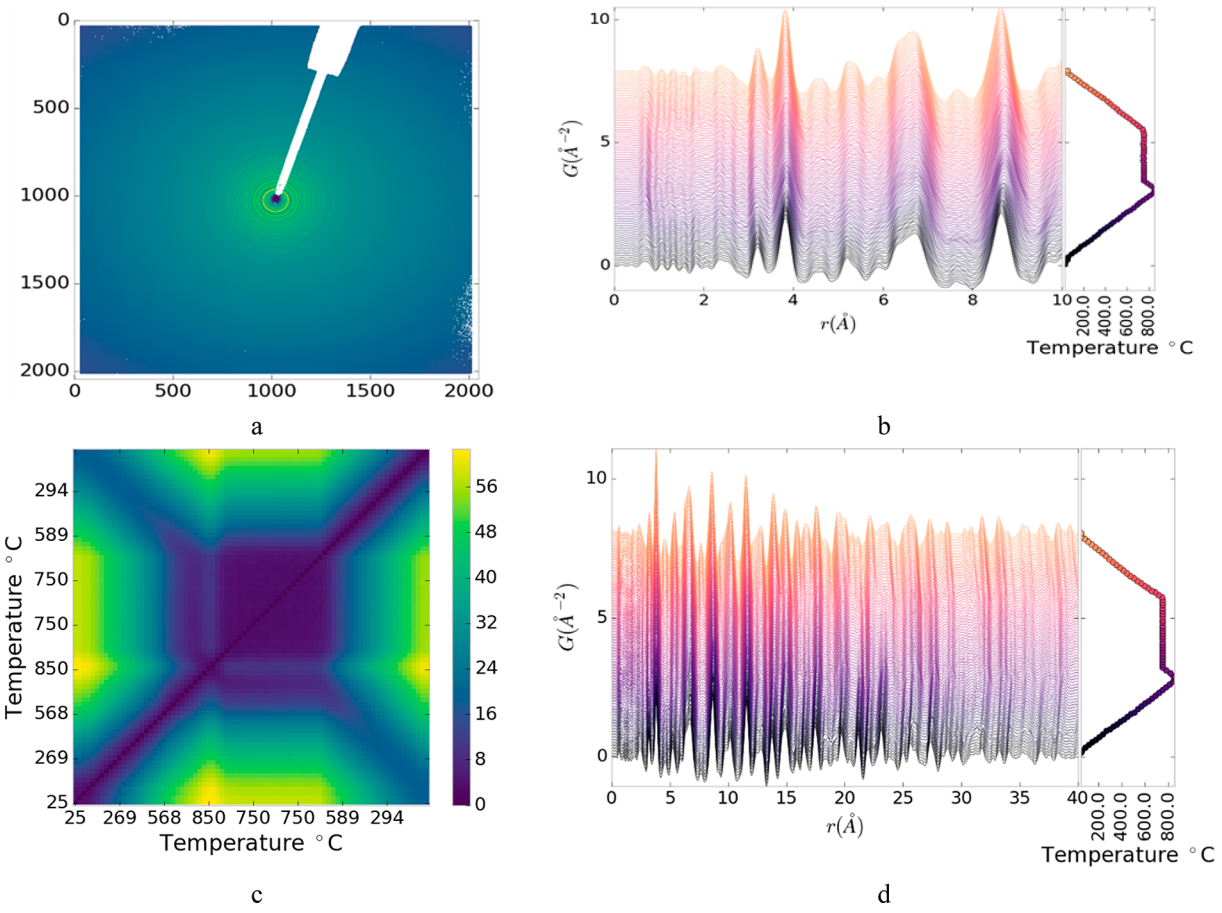

Figure 3. (a) 2D masked data obtained on PNNO powder at 11-ID-B beamline at APS source. Generated PDFs for in situ measurements on PNNO powder for (b) short-range ordering and (c) long-range ordering. Stacked PDF plots correspond to discrete temperature values listed on the right side. (d) Rw distribution (difference in PDF) as a function of temperature

cuprates,[23−25] Cu tends to arrange in a metastable square planar structure at room temperature (RT) but transforms at elevated temperatures to the K_2NiF_4-type structure forming elongated CuO_6 octahedra.[23] Consequently, the focal O atoms on one side of the $(Ni,Cu)O_6$ octahedra tend to tilt away from the adjacent interstitial oxygen site to minimize the oxygen−oxygen Columbic repulsion. However, due to the increase in the distance between the oxygen transport sites, more energy (higher temperature) will be required for further oxygen hopping. As a result of the structural distortion, *i.e.* the oxygen octahedra tilting, some angular strain is produced; this is the most pronounced for the O_e−(Ni,Cu)−O_f arrangement and results in a 3.40% increase in bond angle, as shown in Figure 1b. Simultaneously, the focal O atoms on the opposite side of the $(Ni,Cu)O_6$ octahedra move closer together toward the vacant oxygen interstitial sites and likely reduce their availability for further oxygen transport.[26] These combined steric effects and angle strains in the oxygen octahedra lead to respective changes in the rock-salt layer, thus affecting oxygen ion conduction paths and the concentration of oxygen interstitials.[27]

Conduction of oxygen in PNNO-Cu_y occurs via natural exchange of oxygen atoms between interstitial and apical sites, which allows for oxygen propagation *via* hopping mechanism in the *a*−*b* plane.[26,28] Therefore, obtaining a better understanding of the structural changes in oxygen ion conduction paths is of fundamental importance with respect to the transport properties of the material. Figure 1c shows the refined average (Pr, Nd)−O_e bond lengths. With an increase in Cu content, the overall (Pr,Nd)−O_e bond distance decreases. Considering that the Pr and Nd cations are much heavier than the oxygen ions, they are not expected to be displaced to the same extent. As such, the decrease in bond lengths can be explained by tilting of the oxygen octahedra due to the aforementioned steric and angular strains. A 3.0% decrease in the (Pr,Nd)−O_f bond length (Figure 1d) is even more evident and further indicates the shrinkage of oxygen ion conduction paths, as illustrated in Figure 2b. The largest overall decrease in the (Pr,Nd)−O bond lengths was measured for 5 and 10 mol % Cu doped PNNO.

3.2. In Situ Structural Characterization at the Synchrotron Source. The structural information obtained at room temperature (Section 3.1) was used as a baseline for *in situ* studies. Figure 3a shows an example of a 2D masked data set which was used to generate the PDF plots.[21] The PDFs obtained on the PNNO powder in air during heating and cooling regimes are also shown in Figure 3b−c, at short and long ranges, respectively. Each PDF pattern was collected at a discrete temperature profile, as shown in the inset on the right of each figure panel. Figure 3b shows a short-range PDF which corresponds to atomic distances within a single unit cell, while Figure 3c extends the long-range PDF wherein the atomic distances sample ranges beyond a single unit cell. Each peak in PDF ($G(r)$ plot) represents an atomic pair distance; hence, any shifts in a peak position indicate changes in the distance between any two atoms of interest. The advantage of using

https://doi.org/10.1021/acs.jpcc.2c04006
J. Phys. Chem. C XXXX, XXX, XXX−XXX

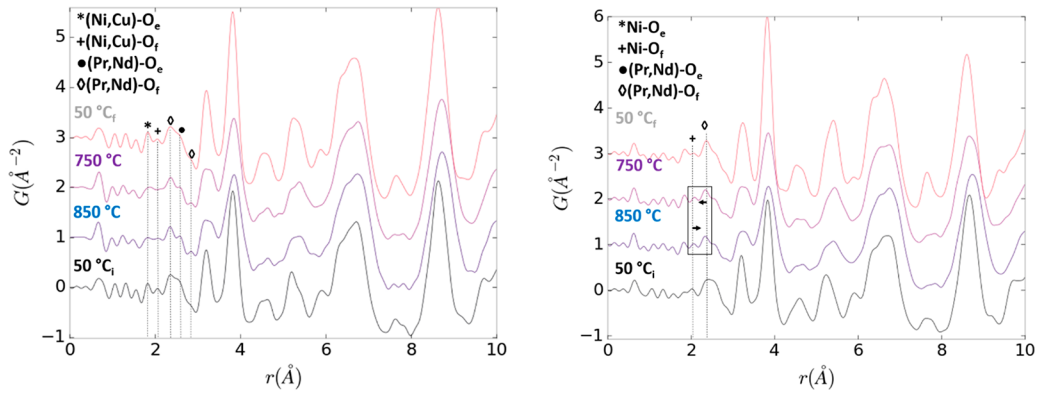

Figure 4. (a) In situ PDF patterns for PNNO(50/50)-Cu_{10} powder at selected temperatures highlighting "frozen" M−O atomic pair distances. (b) In situ PDF patterns on PNNO powder showing changes in M−O distances.

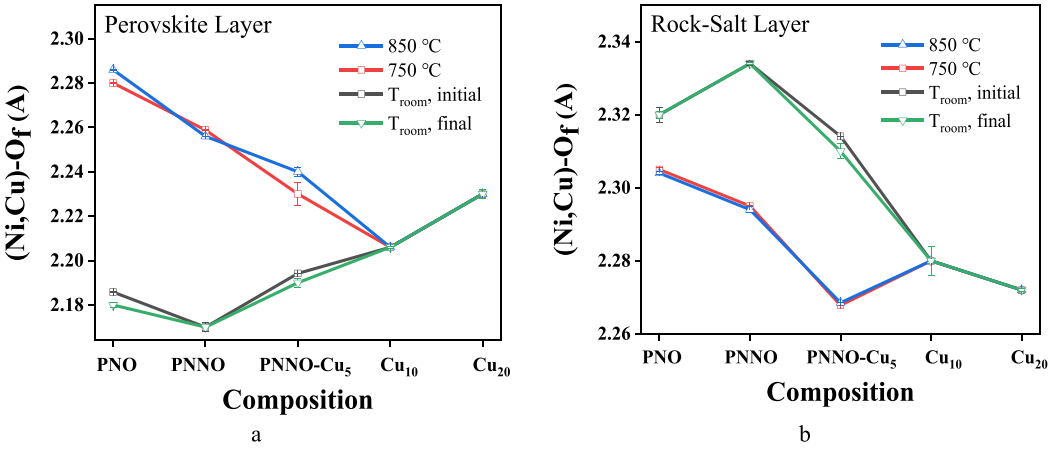

Figure 5. Quantified M−O distances from PDF measurements as a function of composition and temperature for (a) (Ni, Cu)−O_f atomic distance and (b) (Pr, Nd)−O_f atomic distance.

high resolution and high flux synchrotron radiation is that it allows detection of any peak shifts in the measured region to great precision.

At first glance, it appears that the shifts in peak positions are mostly noticeable for metal−metal pairs at r(Å) > 8 (Figure 3b) and for distances longer than a single unit cell (>12.50 Å, Figure 3c). However, a closer examination reveals that significant structural changes occur also at r(Å) < 8. Changes in metal−oxygen (M−O) distances and other structural modifications beyond a single unit cell dimension are not the focus of this study; hence, they will be reported in a separate, future work. However, briefly, the results in Figure 3 reveal that, at atomic distances beyond the single unit cell, various peaks are observed to shift; this observation may indicate turbostratic displacement between the layers, as these are extended structures. At shorter ranges, a general peak shifting occurs during heating to ∼450 °C and is associated with the transition from the orthorhombic to the high temperature tetragonal (HTT) phase.[26,29] Upon cooling, the phase transitioned back to the orthorhombic structure with *Bmab* symmetry. In the temperature window between 450 and 850 °C in air, the peak shifting was not observed, indicating a thermodynamically stable phase, which has been first identified via *in situ* XRD studies on PNNO electrodes in one of our previous works.[15,16]

The relative changes in entire PDF patterns during the heating and cooling regimes were also studied. Figure 3d illustrates the differences in PDFs as a function of temperature. The green/yellow regions indicate larger differences, while blue regions indicate a good match. Substantial differences were observed when comparing low *vs* high temperature PDFs on PNNO-Cu_y. However, during a hold at 750 °C, no changes in the PDFs are observed, indicating the presence of a stable phase. Using this approach, the PDFs at selected temperatures were studied in more detail and compared to results before and after thermal annealing, Figure 4. For any PNNO-Cu_y compositions (Cu_{10} is shown in Figure 4), the metal−oxygen atomic pair distances do not undergo any shifts during thermal annealing, as shown in Figure 4a. The (Ni, Cu)−$O_{f,e}$ and (Pr, Nd)−$O_{f,e}$ distances remain unchanged, indicating rigid octahedra and retained (but also compressed) oxygen ion conduction paths, respectively. Such a stable structure consequently leads to a stabilized phase, as reported in our previous work.[17] In contrast, substantial changes are detected in the PDF patterns of the PNNO composition—*i.e.*, in the absence of Cu but with Nd substituted Pr-sites (Figure 4b), indicating phase transformation.[27] Similarly, the *in situ* PDFs on the PNO powder show substantial changes in M−O distances.

Figure 5 summarizes quantified M−O distances as a function of composition and temperature in the perovskite

https://doi.org/10.1021/acs.jpcc.2c04006
J. Phys. Chem. C XXXX, XXX, XXX−XXX

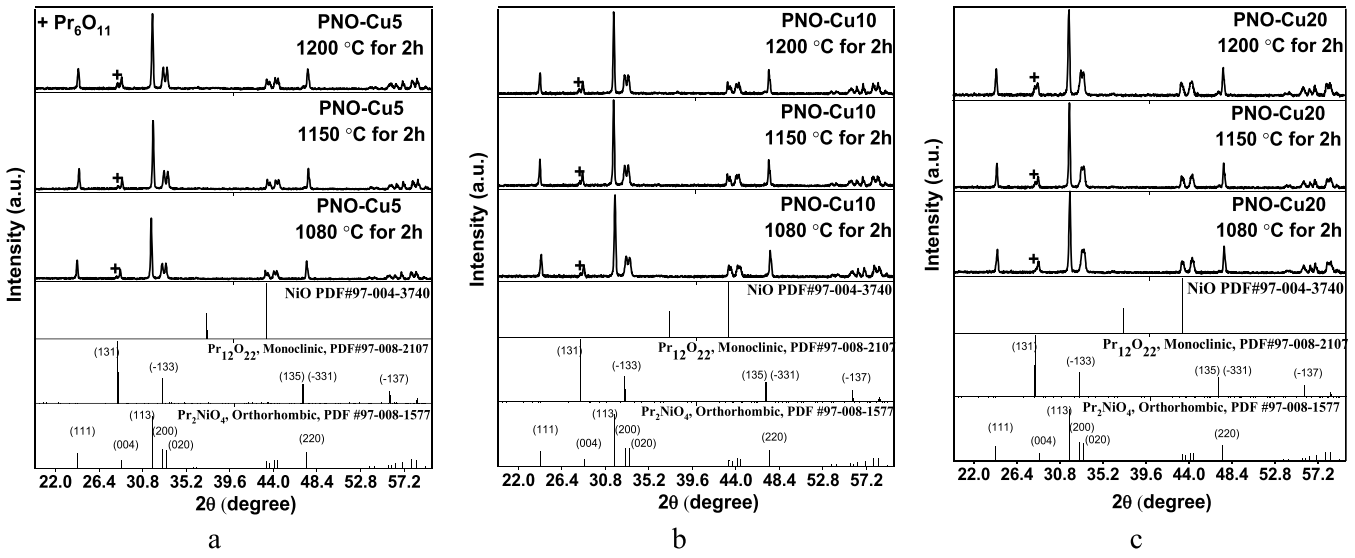

Figure 6. Phase purity in $Pr_2Ni_{1-y}Cu_yO_{4+\delta}$ (PNO-Cu_y) powders (a−c), where y = 0.05, 0.10, and 0.20, respectively. Evolution or PrO_x is marked with (+). Standard XRD patterns are included.

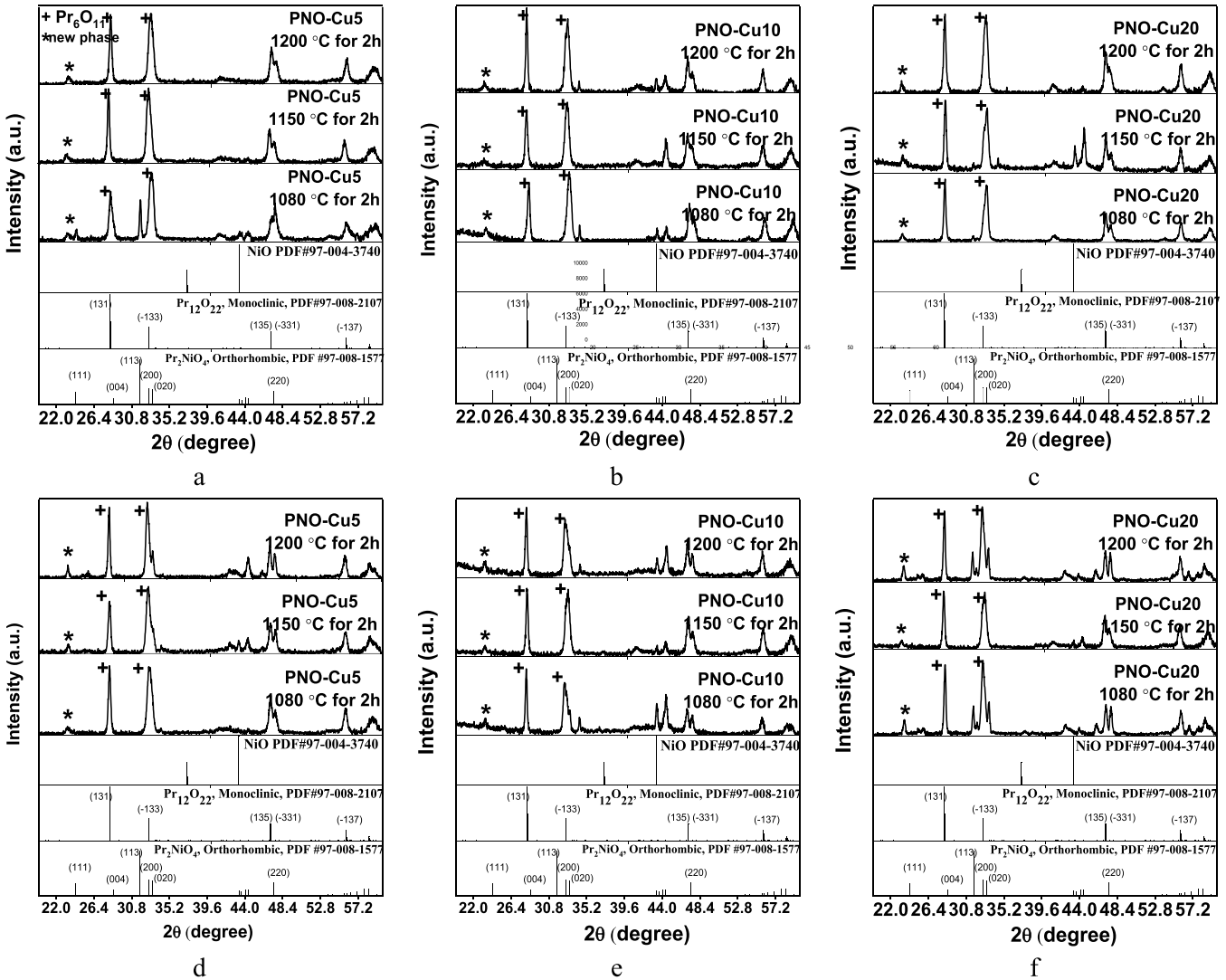

Figure 7. Phase stability in PNO-Cu_y powders after 150-h annealing at 790 °C (a−c) and 870 °C (d−f), where y = 0.05, 0.10, and 0.20, respectively.

https://doi.org/10.1021/acs.jpcc.2c04006
J. Phys. Chem. C XXXX, XXX, XXX−XXX

layer (Figure 5a) and the rock-salt layer (Figure 5b). The largest changes occur in PNO, with a 7% increase in Ni−O_f and 3.2% decrease in Pr−O_f. Such substantial changes in M−O distances can be attributed to a considerable phase transition.[27] In the PNNO composition, the changes are partially suppressed, with a 4% increase and 1.4% decrease in Ni−O_f and Pr−O_f bond lengths, respectively. By contrast for PNNO-Cu_{10} and PNNO-Cu_{20}, the changes are fully suppressed. The results suggest that, with 5% Cu doping, the Cu content is insufficient to stabilize the phase, which still reflects in the somewhat less pronounced changes in the M−O distances. These results are in agreement with a few percent phase transition in PNNO-Cu_5 after long-term operation.[17]

3.3. On the Origin of Structural Changes in Praseodymium Nickelates. The aforementioned structural studies show that phase evolution in praseodymium nickelates is an *in situ* phenomenon and can be linked to changes in the M−O distances in the perovskite and rock-salt layers. However, a question remains as to how a structure can remain "frozen" during the heating process in PNNO-Cu_y, as exemplified by unaltered M−O distances in the PNNO-Cu_{10} and PNNO-Cu_{20} samples. Through molecular dynamics simulations of oxygen transport in PNO, Parfitt *et al.*[26] showed that oxygen diffusivity has a weak dependence on the concentration of oxygen interstitials, which affects the effective migration barrier. In such molecular dynamics studies it was observed that, while an initial increase in oxygen interstitials can increase the diffusion coefficients, this levels off at higher interstitial oxygen concentrations as a result of higher migration barriers. The increase in effective migration barrier was rationalized as the combination of stiffening of the lattice and increased energy of formation of oxygen interstitials. These molecular simulations were in agreement with neutron scattering studies on related K_2NiF_4-type structured materials.[28] Since the cathode materials studied in this work follow the general deintercalation of interstitial oxygen with increase in temperature,[30] then a possible explanation for the retained shrinkage of oxygen ion conduction paths in PNNO(50/50)-Cu_y can be associated with the stiffening of the NiO_6 perovskite layer due to effective pinning of oxygen interstitials.[26] This mechanism accounts for a decreased propensity of the octahedra to tilt, which prevents any further impact on the conduction paths in the rock-salt layer. Furthermore, the Cu^{2+}/Cu^{3+} redox couple may also be responsible for the octahedral stiffening. However, while, in the absence of Cu, the Ni^{2+}/Ni^{3+} redox couple alone cannot suppress structural changes, it is found that high concentrations of Cu dopant (*e.g.*, 30 mol %) may yield an excess of Cu^{3+} which leads to additional strain and hence the inability to refine this particular compound in orthorhombic *Bmab* symmetry. This would explain the narrow concentration range of Cu that can be effectively used to stabilize the phase.

This raises a question as to whether Cu doping on the Ni-site can stabilize the parent PNO phase without Nd substitution on the Pr-site. To answer this question, it is imperative to study the role of Cu-doping in PNO and the long-term phase stability. Obtaining a single orthorhombic phase of PNO-Cu_y with 5, 10, and 20 mol % Cu doping at various temperatures was challenging. In all cases, at least ∼1 mol % of PrO_x was detected during thermal annealing (Figure 6).

The phase transformation occurred in all samples (indicated by the substantial evolution of PrO_x phase) within 150 h at 790 and 870 °C in 3% humidified air (Figure 7). These results reveal that Cu-doping alone is not sufficient in stabilizing the PNO phase. Therefore, we propose that less available Pr cations for oxidation, due to Nd substitution on the Pr-site, and shrinkage in oxygen ion conduction paths, due to Cu-doping on the Ni-site, mutually suppress the formation of PrO_x and phase transition in praseodymium nickelates. Due to the shrinkage of the rock-salt layer (hence, possible decrease in oxygen occupancy)[31] and decrease in (Pr,Nd)−O_f distance, the Pr is less likely to be oxidized and more energy (higher temperature) is required to remove it from the structure. This leaves a very narrow phase transition window, as 1150 °C was the annealing temperature for PNNO-Cu_y. Consequently, the suppressed formation of PrO_x leads to less local stress, due to 68% thermal mismatch, between the two phases and stable long-term phase. Finally, other plausible factors playing into phase stability or occurrence of structural changes may be related to the electronic structure of the material and *p*−*d* orbital interactions between the oxygen atoms in octahedra and the transition metal. Exploring changes in the energy of these orbital interactions may provide insight into stabilized phase and will be addressed in more detail in section 3.4 (Density Functional Theory calculations).

3.4. Density Functional Theory (DFT) Calculations. To obtain a better understanding of the energy of the systems of study, changes in the electronic structure with Cu doping, and the possible origin of the stabilized phase, the density of states (DOS) analysis was performed in PNNO-Cu_y and compared to the baseline compositions (PNO, PNNO). The DFT calculations show that, with an increasing Cu content, the lattice parameters *a* and *b* decrease, while lattice parameter *c* increases. These predictions agree with our PDF analysis. Furthermore, the analysis of M−O_e and M−O_f bond length (M = Cu and Ni) shows that the Cu−O_f is much longer than the Ni−O_f. By contrast, the Cu−O_e is predicted to be slightly shorter than Ni−O_e. These results are consistent with Cu^{2+} having a larger ionic radius than Ni^{2+} (0.73 vs 0.69 Å). Furthermore, upon incorporation of Cu into PNO, the larger ionic radius of Cu^{2+} (cf. Ni^{2+}) results in elongated Cu−O_f distances, which is reflected in the expansion of lattice parameter *c*, and naturally induces some contraction along with the *a* and *b* directions.

Previous results on a similar system have identified a close interplay between the electronic and geometric structures;[32] hence, an attempt was made here to utilize DFT calculations to understand the cause behind the stabilized phase in Cu-doped PNNO. Through detailed electronic structure calculations of La_2NiO_4 nickelate (accompanying XPS experiments), Maiti *et al.*[32] demonstrated that changes in charge-transfer energy are associated with dimensional changes in oxygen octahedra. The NiO_6 octahedra are linked via the corner-sharing of oxygen atoms along with the *x* and *y* directions while being well separated along the *z*-direction (see Figure 2). Therefore, the electronic properties of these systems are controlled by the electronic structure of the two-dimensional network (*ab* plane).[33]

The balanced equation for the substitution of Ni by Cu in PNO is as follows:

$$8Pr_2NiO_4 + Cu = 8Pr_2Ni_{0.875}Cu_{0.125}O_4 + Ni \quad (2)$$

where one Cu atom replaces one of eight Ni-atoms in the perovskite layer. The energy of Cu substitution on the Ni-site was calculated based on eq 3, in which the DFT total energies

https://doi.org/10.1021/acs.jpcc.2c04006
J. Phys. Chem. C XXXX, XXX, XXX−XXX

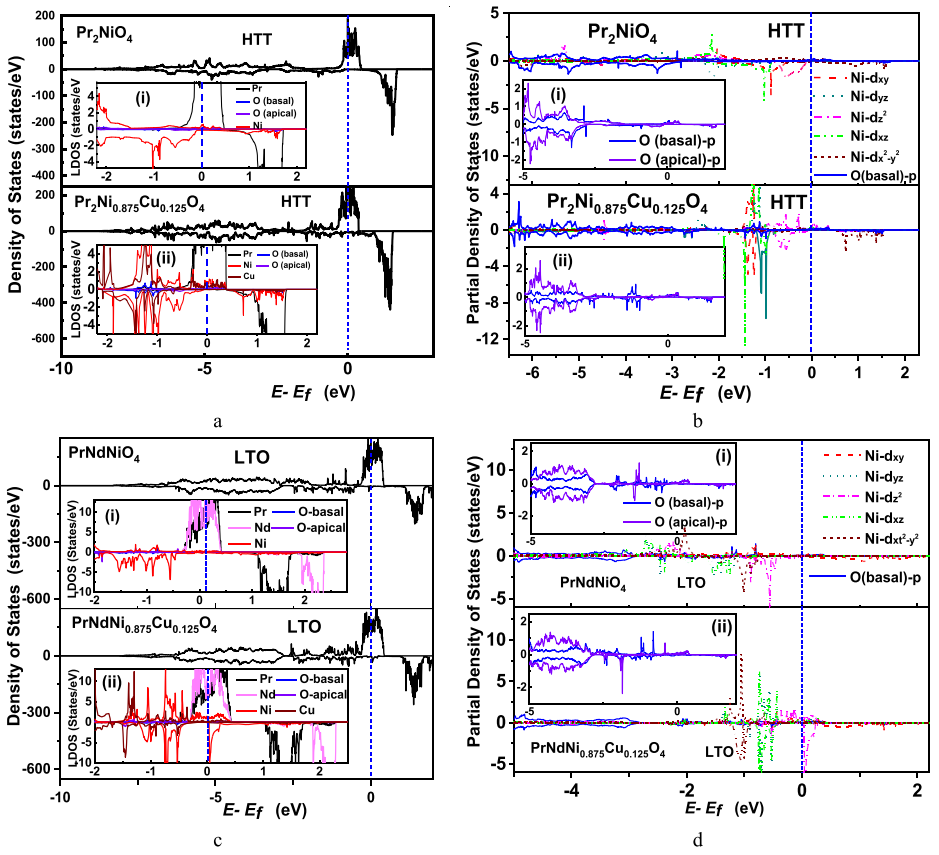

Figure 8. Total and partial density of states (DOS) in the *I*4/*mmm* structure projected onto the atomic orbitals of Pr, Ni, Cu, and O atoms for (a) Pr_2NiO_4 and (b) $Pr_2Ni_{0.875}Cu_{0.125}O_4$. (c) Total density of states for $PrNdNiO_4$ (top panel) and $PrNdNi_{0.875}Cu_{0.125}O_4$ (bottom panel). (d) Partial density of states for $PrNdNiO_4$ (top panel) and $PrNdNi_{0.875}Cu_{0.125}O_4$ (bottom panel).

of ground state Cu and Ni instead of their chemical potentials are used, since they are considered to be equal for most metals without structural transformations at low temperatures.[34]

$$E_{sub} = E_{Pr_2Ni_{0.875}Cu_{0.125}O_4} + E_{Ni} - E_{Pr_2NiO_4} - E_{Cu} \quad (3)$$

where E_{sub} represents the total energy change in the system brought via Cu substitution, while E_{Cu} and E_{Ni} represent the total energies per atom at 0 K for bulk Cu and Ni, respectively. The pure elements are in their standard states; i.e., Cu and Ni both have the fcc crystal structures.

The substitution energy of Cu in PNO with the HTT and LTO phase was calculated to be −1.69 and −1.92 eV/atom, respectively. A similar result (−2.04 eV/atom) was found in the calculation of PNNO, which was performed based on the lattice parameters from experimental work. These negative values of substitution energies suggest that the formation energies of PNO and PNNO cathode materials are higher than those of $Pr_2Ni_{0.875}Cu_{0.125}O_4$ and $PrNdNi_{0.875}Cu_{0.125}O_4$, indicating that these cathode materials with Cu doping are more stable at a certain temperature and oxygen partial pressure.

Figure 8a and b show the total and partial density of states (DOS) in the *I*4/*mmm* structure projected onto the atomic orbitals of Pr, Ni, Cu, and O atoms for Pr_2NiO_4 and $Pr_2Ni_{0.875}Cu_{0.125}O_4$, respectively. Figure 8c, d are the total and partial DOS for $(Pr_{0.5}Nd_{0.5})_2NiO_4$ and $(Pr_{0.5}Nd_{0.5})_2Ni_{0.875}Cu_{0.125}O_4$, respectively. The up-spin DOS (majority spin states) is plotted above zero, and the down-spin DOS (minority spin states), below zero. The dashed line at zero energy is the Fermi level. The most energetically contributing valence orbitals in these compositions are 4*f* on Pr/Nd atoms, 3*d* on Ni/Cu atoms, and 2*p* on O atoms. It can be seen from inset (i) and (ii) in Figure 8a that the contribution of majority 3*d* and 2*p* states just below the Fermi level increased for PNO-Cu_y compared to PNO, indicating the *p*−*d* interaction was strengthened as Cu doped in PNO.

Furthermore, it should be noted that 2*p* states of basal O atoms hybridize strongly with 3*d* states for the Cu-doped system, as shown in the inset (i) and (ii) in Figure 8b, whereas the interaction between 3*d* states of Ni and the apical oxygen states is weak because of the relatively long distance to Ni and O atoms. Similar findings were obtained for the low-temperature orthorhombic phase of Pr_2NiO_4 and $Pr_2Ni_{0.875}Cu_{0.125}O_4$. However, for PNNO(50/50)-Cu_y, 2*p* states of apical and basal oxygen atoms hybridize with the 3*d* states of Ni and Cu atoms around the Fermi level. The partial DOS for the *d* bands of Ni and *p* states of basal oxygen are represented in Figure 8b, d. It clearly reveals that the d_{z^2} band is mainly responsible for the hybridization with 2*p* states. The strengthening of *p*−*d* interaction due to the substitution of Cu for the Ni site and the change in charge-transfer energy leads to higher stability for these kinds of cathode materials.

4. CONCLUSIONS

In this work, we endeavored to identify the origin of structural changes and phase evolution in praseodymium nickelates. The Rietveld refinement and atom pair distribution function at the synchrotron source were utilized to investigate structural changes. The Cu doping on the Ni-site in PNNO leads to

https://doi.org/10.1021/acs.jpcc.2c04006
J. Phys. Chem. C XXXX, XXX, XXX−XXX

formation of steric and angular strain in the perovskite layer resulting in bond elongation between the transition metal and focal oxygen. This bond elongation forces shrinkage in oxygen ion conduction paths in the rock-salt layer, by decreasing the (Pr,Nd)−O_f atomic distance. A strong correlation exists between the shrinkage in oxygen ion conduction paths, phase stability, and electrochemical performance in PNNO-Cu_y. The superior phase stability of PNNO-Cu_y, when compared to PNO, and a wide operating temperature window allow for stable long-term operation in electrochemical cells. The structural approach toward designing active and stable praseodymium nickelate cathodes provides a promising avenue in the development of robust SOFC cathodes.

AUTHOR INFORMATION

Corresponding Authors

Xiao-Dong Zhou − *Department of Chemical Engineering, University of South Carolina, Columbia, South Carolina 29208, United States; Institute for Materials Research and Innovation, Department of Chemical Engineering, University of Louisiana at Lafayette, Lafayette, Louisiana 70504, United States;* orcid.org/0000-0001-9934-9429; Email: zhou@louisiana.edu

Yanxing Zhang − *School of Physics, Henan Normal University, Henan, Xinxiang 453007, China*; Email: zhangyanxing@htu.edu.cn

Guang Tian − *State Key Laboratory for Mesoscopic Physics, School of Physics, Peking University, Beijing 100871, P. R. China*; Email: gtian@pku.edu.cn

Barbara Marchetti − *Institute for Materials Research and Innovation, Department of Chemical Engineering, University of Louisiana at Lafayette, Lafayette, Louisiana 70504, United States;* orcid.org/0000-0002-0661-9029; Email: barbara.marchetti1@louisiana.edu

Authors

Emir Dogdibegovic − *Department of Chemical Engineering, University of South Carolina, Columbia, South Carolina 29208, United States*

Christopher J. Wright − *Department of Chemical Engineering, University of South Carolina, Columbia, South Carolina 29208, United States*

Yudong Wang − *Department of Chemical Engineering, University of South Carolina, Columbia, South Carolina 29208, United States; Institute for Materials Research and Innovation, Department of Chemical Engineering, University of Louisiana at Lafayette, Lafayette, Louisiana 70504, United States*

Qingsheng Cai − *Department of Nuclear Engineering, North Carolina State University, Raleigh, North Carolina 27607, United States*

Shuai Yang − *State Key Laboratory for Mesoscopic Physics, School of Physics, Peking University, Beijing 100871, P. R. China*

Jinbo Yang − *State Key Laboratory for Mesoscopic Physics, School of Physics, Peking University, Beijing 100871, P. R. China;* orcid.org/0000-0003-3517-9701

Complete contact information is available at: https://pubs.acs.org/10.1021/acs.jpcc.2c04006

Notes

The authors declare no competing financial interest.

ACKNOWLEDGMENTS

The authors would like to thank the Department of Energy for the support of this project, under Contracts DE-FE0023475 and DE-EE0009421, and the National Science Foundation under Cooperative Agreement NSF-2119688. The use of the Advanced Photon Source was supported by the U.S. Department of Energy, Office of Science, Office of Basic Energy Sciences, under Contract No. DE-AC02-06CH11357.

REFERENCES

(1) Aleksandrov, K. S.; Beznosikov, B. V. Architecture of Perovskite-Like Crystals. *Crystallogr. Rep.* **1997**, *42*, 556−566.

(2) Beznosikov, B. V.; Aleksandrov, K. S. Perovskite-Like Crystals of the Ruddlesden-Popper Series. *Crystallogr. Rep.* **2000**, *45*, 792−798.

(3) Boehm, E.; Bassat, J. M.; Dordor, P.; Mauvy, F.; Grenier, J. C.; Stevens, P. Oxygen Diffusion and Transport Properties in Non-Stoichiometric $Ln_{2-x}NiO_{4+\delta}$ Oxides. *Solid State Ion.* **2005**, *176*, 2717−2725.

(4) Kovalevsky, A. V.; Kharton, V. V.; Yaremchenko, A. A.; Pivak, Y. V.; Naumovich, E. N.; Frade, J. R. Stability and Oxygen Transport Properties of $Pr_2Nio_{4+\delta d}$ Ceramics. *Journal of European Ceramic Society* **2007**, *27*, 4269−4272.

(5) Yashima, M.; Enoki, M.; Wakita, T.; Ali, R.; Matsushita, Y.; Izumi, F.; Ishihara, T. Structural Disorder and Diffusional Pathway of Oxide Ions in a Doped Pr_2NiO_4-Based Mixed Conductor. *J. Am. Chem. Soc.* **2008**, *130*, 2762−2763.

(6) Grimaud, A.; Mauvy, F.; Bassat, J. M.; Fourcade, S.; Marrony, M.; Grenier, J. C. Hydration and Transport Properties of the $Pr_{2-x}Sr_xNiO_{4+\delta}$ Compounds as H+-Sofc Cathodes. *J. Mater. Chem.* **2012**, *22*, 16017−16025.

(7) Frayret, C.; Villesuzanne, A.; Pouchard, M. Application of Density Functional Theory to the Modeling of the Mixed Ionic and Electronic Conductor La2nio4+Delta: Lattice Relaxation, Oxygen Mobility, and Energetics of Frenkel Defects. *Chem. Mater.* **2005**, *17*, 6538−6544.

(8) Druce, J.; Tellez, H.; Hyodo, J. Surface Segregation and Poisoning in Materials for Low-Temperature Sofcs. *MRS Bull.* **2014**, *39*, 810−815.

(9) Minervini, L.; Grimes, R. W.; Kilner, J. A.; Sickafus, K. E. Oxygen Migration in $La_2NiO_{4+\delta}$. *J. Mater. Chem.* **2000**, *10*, 2349−2354.

(10) Chen, Y. B.; Zhou, W.; Ding, D.; Liu, M. L.; Ciucci, F.; Tade, M.; Shao, Z. P. Advances in Cathode Materials for Solid Oxide Fuel Cells: Complex Oxides without Alkaline Earth Metal Elements. *Adv. Energy Mater.* **2015**, *5*, 1500537.

(11) Yashima, M.; Sirikanda, N.; Ishihara, T. Crystal Structure, Diffusion Path, and Oxygen Permeability of a Pr_2NiO4-Based Mixed Conductor $(Pr_{0.9}La_{0.1})_2(Ni_{0.74}Cu_{0.21}Ga_{0.05})O_{4+\delta}$. *J. Am. Chem. Soc.* **2010**, *132*, 2385−2392.

(12) Gao, Z.; Mogni, L. V.; Miller, E. C.; Railsback, J. G.; Barnett, S. A. A Perspective on Low-Temperature Solid Oxide Fuel Cells. *Energy Environ. Sci.* **2016**, *9*, 1602−1644.

(13) Geffroy, P. M.; Reichmann, M.; Chartier, T.; Bassat, J. M.; Grenier, J. C. Evaluating Oxygen Diffusion, Surface Exchange and Oxygen Semi-Permeation in $Ln_2NiO_{4+\delta}$ Membranes (Ln = La, Pr and Nd). *J. Membr. Sci.* **2014**, *451*, 234−242.

(14) Dogdibegovic, E.; Guan, W.; Yan, J.; Cheng, M.; Zhou, X.-D. Activity and Stability of $(Pr_{1-x}Nd_x)_2NiO_4$ as Cathodes for Solid Oxide Fuel Cells: II. Electrochemical Performance and Performance Durability. *J. Electrochem. Soc.* **2016**, *163*, F1344−F1349.

(15) Dogdibegovic, E.; Alabri, N. S.; Wright, C. J.; Hardy, J. S.; Coyle, C. A.; Horlick, S. A.; Guan, W. B.; Stevenson, J. W.; Zhou, X. D. Activity and Stability of $(Pr_{1-x}Nd_x)_2NiO_4$ as Cathodes for Solid Oxide Fuel Cells: Part V., In Situ Studies of Phase Evolution. *J. Electrochem. Soc.* **2017**, *164*, F1115−F1121.

(16) Dogdibegovic, E.; Wright, C. J.; Zhou, X. D. Stability and Activity of $(Pr_{1-x}Nd_x)_2NiO4$ as Cathodes for Solid Oxide Fuel Cells: I., Quantification of Phase Evolution in Pr_2NiO_4. *J. Am. Ceram. Soc.* **2016**, *99*, 2737−2741.

https://doi.org/10.1021/acs.jpcc.2c04006
J. Phys. Chem. C XXXX, XXX, XXX−XXX

(17) Dogdibegovic, E.; Yan, J. B.; Cai, Q. S.; Jung, H. Y.; Xing, Z. L.; Liu, Z. E.; Goettler, R. W.; Zhou, X. D. Activity and Stability of $(Pr_{1-X}Nd_x)_2NiO_{4+\delta}$ as Cathodes for Oxide Fuel Cells: Part Vi. The Role of Cu Dopant on the Structure and Electrochemical Properties. *J. Electrochem. Soc.* **2017**, *164*, F3131−F3139.
(18) Dogdibegovic, E.; C, J. W.; Zhou, X.-D. Stability and Activity of $(Pr_{1-X}Nd_x)_2NiO_4$ as Cathodes for Solid Oxide Fuelcells: I. Quantification of Phase Evolution in Pr_2NiO_4. *J. Am. Ceram. Soc.* **2016**, 1−5.
(19) Chick, L. A.; Pederson, L. R.; Maupin, G. D.; Bates, J. L.; Thomas, L. E.; Exarhos, G. J. Glycine Nitrate Combustion Synthesis of Oxide Ceramic Powders. *Mater. Lett.* **1990**, *10*, 6−12.
(20) Dogdibegovic, E.; Cai, Q.; James, W. J.; Yelon, W. B.; Anderson, H. U.; Yang, J.-B.; Zhou, X.-D. Coupling between Magnetic Exchange and Charge Activation in Cu-Doped $LaFeO_3$. *J. Am. Ceram. Soc.* **2016**, *99*, 2035−2039.
(21) Coduri, M.; Scavini, M.; Brunelli, M.; Masala, P. In Situ Pair Distribution Function Study on Lanthanum Doped Ceria. *Phys. Chem. Chem. Phys.* **2013**, *15*, 8495−8505.
(22) Chupas, P. J.; Chapman, K. W.; Kurtz, C.; Hanson, J. C.; Lee, P. L.; Grey, C. P. A Versatile Sample-Environment Cell for Non-Ambient X-Ray Scattering Experiments. *J. Appl. Crystallogr.* **2008**, *41*, 822−824.
(23) Hord, R.; Cordier, G.; Hofmann, K.; Buckow, A.; Pascua, G.; Luetkens, H.; Alff, L.; Albert, B. Transitions between Lanthanum Cuprates: Crystal Structures of T', Orthorhombic, and K_2NiF_4-Type La_2CuO_4. *Z. Anorg. Allg. Chem.* **2011**, *637*, 1114−1117.
(24) Grande, B.; Müller-Buschbaum, Hk.; Schweizer, M. *Anorg. Allg. Chem.* **1977**, *428*, 120−124.
(25) Muller-Buschbaum, H.; Wollschlager, Z. Z. *Anorg. Allg. Chem.* **1975**, *414*, 76−80.
(26) Parfitt, D.; Chroneos, A.; Kilner, J. A.; Grimes, R. W. Molecular Dynamics Study of Oxygen Diffusion in $Pr_2NiO_{4+\delta}$. *Phys. Chem. Chem. Phys.* **2010**, *12*, 6834−6836.
(27) Dogdibegovic, E.; Alabri, Q. C. N. S.; Guan, W.; Zhou, X.-D. Activity and Stability of $(Pr_{1-X}Nd_x)_2NiO_4$ as Cathodes for Solid Oxide Fuel Cells: IIICrystal Structure, Electrical Properties, and Micro-structural Analysis. *J. Electrochem. Soc.* **2017**, *164*, F99.
(28) Yashima, M.; Enoki, M.; Wakita, T.; Ali, R.; Matsushita, Y.; Izumi, F.; Ishihara, T. Structural Disorder and Diffusional Pathway of Oxide Ions in a Doped Pr_2NiO_4-Based Mixed Conductor. *J. Am. Chem. Soc.* **2008**, *130*, 2762.
(29) Broux, T.; Prestipino, C.; Bahout, M.; Paofai, S; Elkaïm, E.; Vibhu, V.; Grenier, J.-C.; Rougier, A.; Bassat, J.-M.; Hernandez, O. Structure and Reactivity with Oxygen of $Pr_2NiO_{4+\delta}$: an In Situ Synchrotron X-Ray Powder Diffraction Study. *Dalton Trans.* **2016**, *45*, 3024−3033.
(30) Boehm, E.; Bassat, J. M.; Dordor, P.; Mauvy, F.; Grenier, J. C.; Stevens, P. Oxygen Diffusion and Transport Properties in Non-Stoichiometric $Ln_{2-X}NiO_{4+\delta}$ Oxides. *Solid State Ion.* **2005**, *176*, 2717−2725.
(31) Boehm, E.; Bassat, J. M.; Steil, M. C.; Dordor, P.; Mauvy, F.; Grenier, J. C. Oxygen Transport Properties of $La_2Ni_{1-X}Cu_xO_{4+\delta}$elta Mixed Conducting Oxides. *Solid State Sci.* **2003**, *5*, 973−981.
(32) Maiti, K.; Mahadevan, P.; Sarma, D. D. Evolution of Electronic Structure with Dimensionality in Divalent Nickelates. *Phys. Rev. B* **1999**, *59*, 12457−12470.
(33) Mahadevan, P.; Sheshadri, K.; Sarma, D. D.; Krishnamurthy, H. R.; Pandit, R. Electronic and Magnetic Transitions in a Multiband Model for La_2NiO_4. *Phys. Rev. B* **1997**, *55*, 9203−9206.
(34) Emery, A. A.; Wolverton, C. High-Throughput DFT Calculations of Formation Energy, Stability and Oxygen Vacancy Formation Energy of ABO_3 Perovskites. *Scientific Data* **2017**, *4*, 170153.

https://doi.org/10.1021/acs.jpcc.2c04006
J. Phys. Chem. C XXXX, XXX, XXX−XXX